Combined Raman Spectroscopic and Theoretical Investigation of Fundamental Vibrational Bands of Furfuryl Alcohol (2-furanmethanol)

S. Barsberg*,† and R. W. Berg‡

The Royal Veterinary and Agricultural University, Forest and Landscape, Rolighedsvej 23, DK-1958 Frederiksberg C, Denmark, and Technical University of Denmark, Department of Chemistry, Kemitorvet, B. 207, DK-2800 Lyngby, Denmark

Received: March 16, 2006; In Final Form: June 2, 2006

Furfuryl alcohol (FA) is a promising reactive precursor for new materials. FA reaction mechanisms, that is, self-reactions or cross reactions with other substances, can be studied by vibrational spectroscopy. We present a necessary prerequisite for such studies by a Raman spectroscopic and theoretical study of FA in weakly interacting environments. It is the first study of FA vibrational properties based on density functional theory (DFT/B3LYP), and a recently proposed hybrid approach to the calculation of fundamental frequencies, which also includes an anharmonic contribution. FA occupies five different conformational states, each with more than 5% probability, and two of these dominate at $T = 298$ K. Excluding one frequency, the remaining ones are predicted as a weighted average over the two dominant conformers to a best RMS error of 8 cm^{-1} and are qualitatively assigned. The excluded CH stretching mode is underestimated by 65 cm^{-1}. This may be due to a combination of an insufficient level of theory and the neglect of Fermi interactions for properly describing this type of mode.

Introduction

The vegetal biomass constitutes an enormous renewable source of chemicals. These can be original biomass constituents, that is, starch, hemicelluloses, cellulose, and lignin, or products derived from these. Biomass-based chemicals can provide original polymers, which are not readily available via petroleum-based chemistry. An interesting example is furfuryl alcohol (FA), which is industrially produced via conversion from furfural, which is derived from plant sources. In the presence of an acidic catalyst, FA undergoes a thermally activated polycondensation process, which leads to linear and branched polymers. Several different mechanisms govern this complex process, which leads to progressive coloration and resinification.[1−5]

This reactivity of FA is also utilized in a promising process which substitutes conventional wood impregnation with a potentially environmentally safe alternative.[6,7] The raw wood is first co-impregnated with FA and an acidic catalyst. The impregnated wood is heated, and FA then reacts within the wood cell wall or lumens. The last curing step is not well understood but is likely to involve both self-condensation reactions of FA as well as cross-condensation reactions between FA and wood cell wall components.

These reactions can be studied using vibrational (IR and Raman) spectroscopy, which provides molecular "fingerprints" and thus information on the reaction products as well as on their origins. The interpretation of vibrational bands is strengthened by application of quantum chemical calculations for predicting normal mode vibrations of appropriate molecular models. Natural choices of such models are (unreacted) FA and oligomeric structures derived either from FA or from both FA and a model of a cell wall component. The potential of vibrational spectroscopy for providing detailed chemical knowledge of FA reactions—as NMR spectroscopy would be more commonly used for—can be much improved by recently introduced frequency calculation methods. These are feasible for relatively large molecular systems without any prior empirical knowledge (which enters into, for example, frequency scaling factors), and at the same time they provide very good prediction errors for fundamental bands of typically <10 cm^{-1}. In the present work, we test such a method for FA for the first time and compare the results with experimental band positions. It thus provides a reference for future work on FA reaction products and their vibrational properties.

The conformational properties of FA complicate the thermodynamics and vibrational properties. In analogy with allylic alcohols the C═C−C−O−H chain leads to different conformational states distinguished by the 3C═4C−9C−12O and 4C−9C−12O−13H dihedral angles.[8] Previous MP2/6-31G(d) work identified five different FA conformations, and microwave spectroscopy indicated that two of these dominate in the gas phase at room temperature.[9] In principle, any reaction of FA is initiated from all of these five different (thermally populated) initial states, and reaction rates can differ between these five reaction channels.

The present work focuses on thermodynamic and vibrational properties of FA in the gas phase or weakly interacting solution. It was recently shown that the combination of harmonic and anharmonic frequency calculations using density functional theory (DFT) provides unambiguous assignments of vibrational bands with <10 cm^{-1} average prediction error for reported cases.[10−15] Each frequency is obtained—without use of a scaling procedure—as the sum of a harmonic large basis set frequency and an anharmonic small basis set correction (obtained by a perturbative treatment[16]), henceforth referred to as a *hybrid* calculation.

* Corresponding author. Phone: +45 35 28 16 86. Fax: +45 35 28 15 08. E-mail: sbar@kvl.dk.
† The Royal Veterinary and Agricultural University.
‡ Technical University of Denmark.

10.1021/jp061642x CCC: $33.50
Published on Web 07/08/2006

We report a combined Raman spectroscopic and theoretical investigation of fundamental vibrational bands of FA. The different conformers of FA and their population probabilities at $T = 298$ K are estimated using DFT. Vibrational band assignments and positions are derived from hybrid DFT frequency calculations and compared with the experimental results.

Experimental Section

Furfuryl alcohol ($C_5H_6O_2$) was obtained from Sigma-Aldrich and distilled twice before use. Toluene (>99.5%) was obtained from Bie & Berntsen, and carbon tetrachloride (>99.5%) and benzonitrile (>99%) were obtained from Fluka.

Raman spectra were obtained by use of a DILOR-XY 800-mm focal length multichannel spectrometer with horizontal Ar^+-ion laser excitation (514.5 nm, ~300 mW, vertically polarized and with the argon plasma lines filtered off with an interference filter). Rayleigh scattered light was filtered off with a double pre-monochromator (with slit widths 200, 2000, and 200 μm). The Raman light was obtained in a 90° scattering configuration and dispersed by use of an 1800 lines/mm grating and focused onto a CCD detector, cooled by liquid nitrogen to 140 K. The spectral resolution was approximately 4 cm^{-1}.

Spectra were obtained first from 1 mL of solvent (toluene or carbon tetrachloride)—providing a background spectrum—then from the same vial into which FA was repeatedly added and mixed in vol/vol concentrations of 1.0, 2.1, 6.6, and 13.1%, respectively. Spectra of benzonitrile were obtained at six evenly dispersed time intervals throughout the whole measurement period and used for frequency calibration following the ASTM E 1840 standard.[17,18]

Frequency errors were obtained from combining (1) the published errors (standard deviation) of the ASTM E 1840 standard, (2) the frequencies standard deviation of benzonitrile bands derived from the six spectra, and (3) the errors of the functional profile fit to experimental bands.

A corrected FA spectrum $I_C(\nu)$ was obtained by subtracting an appropriately scaled background solvent spectrum $I_S(\nu)$ and a relatively weak structure less fluorescence background $I_F(\nu)$ from the raw spectrum $I(\nu)$, that is, $I_C(\nu) = I(\nu) - (f(\nu) \times I_S(\nu)) - I_F(\nu)$. By observing the intensity change of characteristic solvent peaks—comparing $I_S(\nu)$ and $I(\nu)$—it was found that the scaling constant should include a weak linear dependence $f(\nu) = A + B\nu$ on the wavenumber ν. The constants A and B were determined by linear fitting. Spectral information from benzonitrile spectra or corrected FA spectra, for example, band center frequencies, was obtained from fitting *single* Gaussian or Lorenzian profiles to well-separated bands and *multiple* profiles to partly overlapping bands.

The software package Gaussian03 was used for predicting molecular properties of FA using density functional theory, that is, the B3LYP functional, combined with the standard basis sets: 6-31G(d), 6-31G(d,p), 6-311++G(2df,2p), cc-pVTZ, and AUG-cc-pVTZ, where the three last are referred to as "B1", "B2", and "B2a", respectively.[19] Conformational states were searched for by performing relaxed scans using the relatively inexpensive 6-31G(d) basis set, where the two dihedral angles Φ_1(3C=4C−9C−12O) and Φ_2(4C−9C−12O−13H), determining the OH group position (see Figure 1), were varied. Structures relatively close to a local energy minimum were then subjected to full unconstrained geometry optimization.

The conformational states thus obtained were each fully optimized using all other basis sets as well. The occupational probability p_i of each conformer (i) is derived from the Gibbs distribution, that is, $p_i = A \exp(G_i/k_BT)$, where $G_i = H_i - TS_i$ is the free energy of conformer (i), A derives from $\sum_i p_i = 1$, and k_B is the Boltzmann constant. For each conformer and basis set, a harmonic frequency calculation was performed at the optimized structure. An anharmonic frequency calculation was performed for the two lowest-energy conformers as well using the 6-31G(d,p) basis set. Reported Raman and IR intensities were calculated using the B1 basis set.

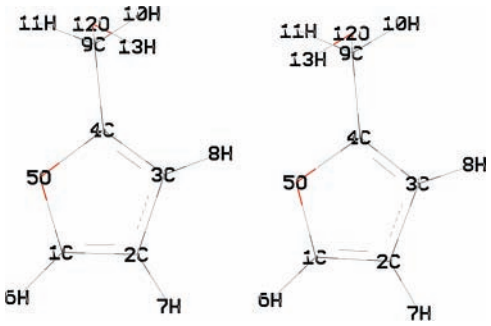

Figure 1. The FA *Skew 1* (left) and *Skew 3* (right) conformers.

As a reference for the DFT calculations, the five conformers obtained as fully optimized B3LYP/B2a structures were each subjected to a MP2/B2a single-point calculation. In addition, the alcohol part of furfuryl alcohol, that is, the normal modes localized on this part of the molecule, was modeled by methanol. As a reference for the anharmonic frequency calculations, the methanol structure was fully optimized at the B3LYP/6-31G-(d,p) and MP2/6-31G(d,p) levels, and B3LYP or MP2 anharmonic frequency calculations were performed for the optimized structures using the same basis set.

Results

The band position difference derived from fitting the same band with Lorenzian or Gaussian profiles was insignificant relative to other error sources, and for strong bands amounted typically to <0.02 cm^{-1}. Thus, the frequency error was derived in most cases by and large from the ASTM E 1840 standard combined with the instrumental repeatability error, which in total amounted to ~1 cm^{-1} across the spectrum. The most intense solvent bands exclude a reliable detection of some FA bands. This is depicted in Figure 2, where intense CCl_4 bands at 220, 315, 460, 760, and 790 cm^{-1} exclude detection of FA bands (and give rise to very "noisy" intervals), whereas the weak and broad 1530 cm^{-1} CCl_4 band poses no problem. The very strong FA 1500 cm^{-1} band peaks at *Y*-axis values out-of-scale at ~440, ~950, and ~33000 (neat liquid FA). The weak peak in one of the spectra at 3470 cm^{-1} is a nonreproducible artifact. A weak fluorescence background, increasing toward higher wavenumbers, is also noted.

FA band positions differed little between the two solvents (average absolute difference ~ 2 cm^{-1}), and since most bands could be detected using CCl_4 we present the positions obtained in this solvent except for a few cases where these were reliably obtained only in toluene. For a few bands, a concentration dependence of their position was observed. This was then extrapolated to the infinite dilution limit (assuming the wavenumber shift to be linear in concentration). In Table 2 we list all observable experimental fundamental frequencies together with the DFT results, which will be explained below.

The spectrum of the neat liquid FA (Figure 2c) clearly exhibits a few very weak bands (at positions very close to the predicted ones), which cannot be observed in the diluted samples. However, the neat liquid (FA "dissolved" in FA)

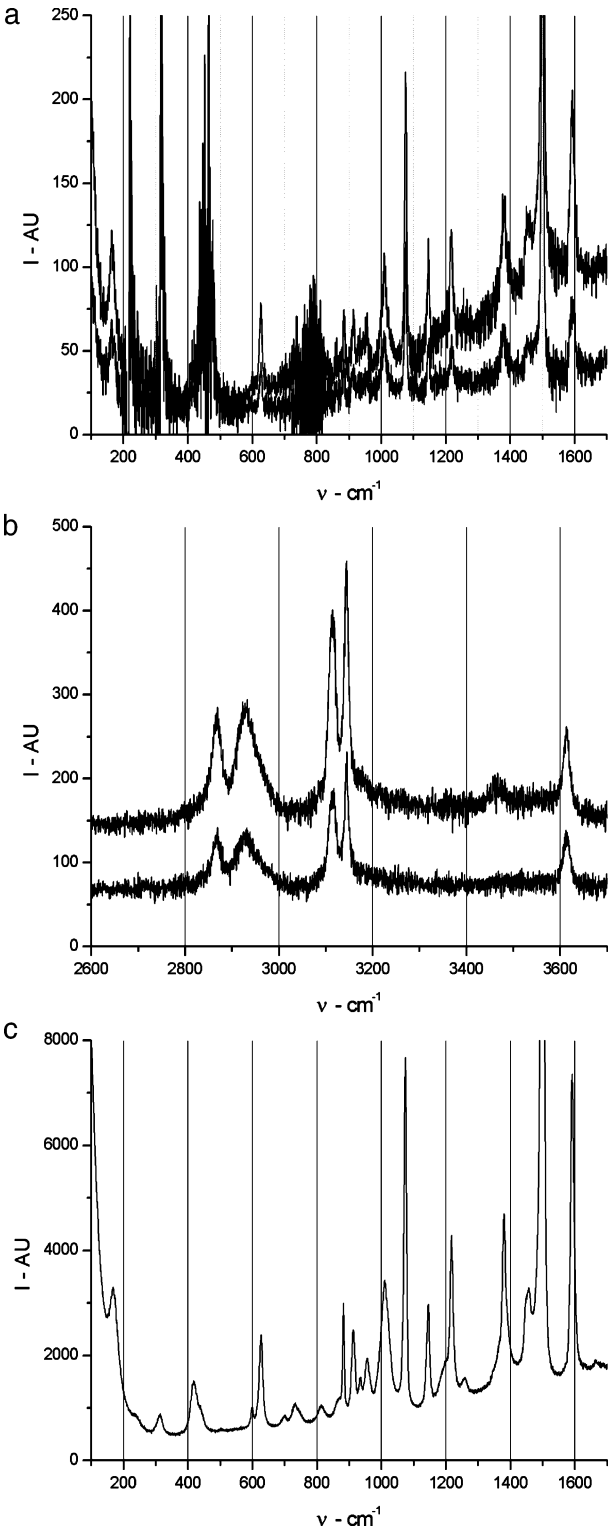

Figure 2. Raman spectra of (a,b) 1% and 2.1% FA in CCl_4 corrected for the solvent, and of (c) the neat liquid FA.

cannot be taken as representative for a weakly interacting environment. Therefore these weak bands are necessarily excluded from this study.

In accordance with previous findings, five conformational FA states were determined by the B3LYP/6-31G(d) search.[9] The absence of imaginary frequencies for all conformers and basis sets confirmed these to represent true energy minima. For ease of comparison we adopt the skew/syn notation used previously for a qualitative distinction between the conformers. In the syn conformation the C═C−C−O atoms are coplanar, whereas the C−O bond forms an angle of ∼120° with the C═C−C plane in the skew form. In the following, all references to MP2 results refer to the same work.[9]

TABLE 1: Selected Structural Parameters, Dipole Moments (μ), Relative Free Energies (ΔG), and Occupational Probabilities (p_i) at T = 298 K of the Five Conformers Derived by B3LYP Calculations and the Large Basis Sets B1, B2, and B2A[a]

	conformer				
	Skew 1	*Skew 2*	*Skew 3*	*Syn 1*	*Syn 2*
Φ_1 B2a	**107.4**	**104.0**	**105.9**	**22.6**	**0.0**
B2	108.2	105.1	106.5	20.7	0.0
B1	107.5	104.0	106.2	22.5	0.0
Φ_2 B2a	**−52.6**	**168.7**	**59.7**	**58.4**	**180.0**
B2	−53.2	167.0	59.9	58.7	180.0
B1	−52.7	168.2	59.3	58.2	180.0
$d(O_F-H_{Me})$ B2a	**3.304**	**3.823**	**2.789**	**3.736**	**4.342**
B2	3.291	3.800	2.769	3.739	4.339
B1	3.305	3.819	2.785	3.735	4.341
μ B2a	**2.247**	**1.566**	**1.613**	**1.346**	**1.210**
B2	2.118	1.492	1.523	1.318	1.262
B1	2.296	1.599	1.655	1.384	1.242
ΔG B2a	**42.7**	**175.7**	**0.0**	**133.4**	**197.1**
B2	37.9	200.5	0.0	91.2	147.3
B1	45.0	184.6	0.0	133.6	152.8
p B2a	**0.295**	**0.072**	**0.463**	**0.113**	**0.057**
B2	0.281	0.050	0.420	0.160	0.088
B1	0.282	0.064	0.454	0.110	0.090

[a] ΔG is relative to the free energy of the *Skew 3* conformer. The units used are degrees, Å, Debye, and 10^{-5} Hartree. The largest basis set B2A results are emphasized in bold.

The absolute deviations averaged over all conformers of (Φ_1, Φ_2) between the B3LYP/B2a and the MP2/6-31G(d) results are $(\Delta\Phi_1, \Delta\Phi_2)_{AV}$ = (3.7°, 2.8°), whereas those between B3LYP/B2a and B3LYP/B2 or B3LYP/B1 are (0.9°, 0.6°) and (0.1°, 0.2°), respectively. The largest discrepancy arises from the *Syn 2* (Φ_1, Φ_2) values, which equal (10°, 173°) for the MP2 calculations and (0°, 180°) for the B3LYP calculations. The B3LYP results for *Syn 2* were confirmed by starting full unconstrained geometry optimizations from geometries which were the results of partial optimizations using the dihedral constraints (Φ_1, Φ_2) = (10°, 173°). This led to a monotonic energy decrease until the minimum at (0°, 180°) was attained. Selected properties are listed in Table 1 together with the occupational probability of each conformer. The energies of the MP2/B2a single-point calculations were each combined with the zero-point energy and thermal corrections obtained from the B3LYP/B2a calculation. This resulted in (hybrid) ΔG values close to those of the pure B3LYP/B2a calculation (listed in Table 1) of *Skew 1*: 41.3, *Skew 2*: 187.6, *Skew 3*: 0, *Syn 1*: 143.0, and *Syn 2*: 226.0 (units: 10^{-5} Hartree). Thus, all results indicate a predominant occupation of the *Skew 1* and *Skew 3* conformers.

The calculated vibrational properties of FA should be represented by a weighted superposition of those of the individual conformers. Since the Raman spectra do not convincingly exhibit resolved bands assignable to the two dominant conformers, the relevant calculated frequencies can for each normal mode be obtained either (1) from the lowest energy *Skew 3* conformer (neglecting all other conformers) or more appropriately (2) from a frequency ν_{Calc} obtained as a weighted average of the two (usually close-lying) calculated frequencies $\nu_{Calc}(1)$ and $\nu_{Calc}(2)$ for each of the two lowest energy conformers *Skew 1* and *Skew 3*, respectively. Each of the two weight factors is obtained as the B3LYP/B2a occupational probability p_i multiplied by the calculated Raman intensity $R(i)$. Thus the average frequency is $\nu_{Calc} = (R(1)p_1 \times \nu_{Calc}(1) + R(2)p_2 \times \nu_{Calc}(2))/(R(1)p_1 + R(2)p_2)$.

TABLE 2: Experimental and Hybrid B2//6-31G(d,p) Frequencies and Assignments for the Two Lowest Energy Conformers[a]

		Skew 3			*Skew 1*			
no.	expt	calcd	R	IR	calcd	R	IR	assignment
33	3623	3630.8	0.511	0.311	3615.6	0.647	0.231	Me−OH str
32	3153	3141.7	1.208	0.001	3140.1	1.228	0.001	F−CH str
31	3123	3116.8	0.639	0.002	3110.6	0.651	0.003	F−CH str
30	3123	3114.1	0.746	0.025	3107.8	0.695	0.028	F−CH str
29	2935	2964.1	0.636	0.108	2936.9	0.997	0.125	Me−CH str
28	2874	2770.5	1.432	0.389	2858.1	1.076	0.374	Me-CH str
27	1598	1596.9	0.204	0.007	1584.9	0.204	0.014	F−CC str
26	1504	1496.5	1.000	0.106	1495.7	1.052	0.126	F−CC str
25	1459	1455.4	0.073	0.024	1458.5	0.095	0.025	Me−CH bend
24	1385	1383.2	0.135	0.001	1387.9	0.163	0.165	F−CC/CO str
23	NO	1373.3	0.041	0.520	1376.6	0.065	0.421	Me−CH/OH bend
22	NO	1327.7	0.082	0.032	1317.3	0.017	0.028	Me−CH/OH bend
21	NO	1244.3	0.016	0.078	1238.4	0.012	0.076	collective
20	1221	1210.8	0.129	0.198	1215.2	0.137	0.075	F−CC/CO str Me−CC str
19	NR	1151.4	0.010	0.296	1159.0	0.056	0.152	collective
18	1150	1145.3	0.042	0.053	1150.7	0.057	0.266	collective
17	1079	1078.4	0.134	0.042	1083.2	0.117	0.047	F−CO str F−CH ip bend
16	NR	1009.5	0.028	0.213	1008.4	0.011	0.122	F−CH ip bend
15	1012	1001.8	0.149	1.000	1008.0	0.135	0.960	Me−CO str
14	951 ± 2	959.2	0.035	0.044	945.9	0.060	0.342	collective
13	915	904.5	0.027	0.393	913.1	0.024	0.167	collective
12	886	893.7	0.036	0.076	893.6	0.038	0.051	F−CCC ip bend
11	863	873.9	0.010	0.003	872.3	0.008	0.011	F−CH op bend
10	816*	817.9	0.010	0.119	818.4	0.011	0.126	F−CH op bend
9	735*	745.7	0.004	0.555	745.3	0.005	0.605	collective F−CH op bend
8	735*	731.3	0.007	0.176	733.2	0.007	0.106	collective F−CH op bend
7	628	632.5	0.037	0.049	631.6	0.036	0.055	collective
6	600	609.2	0.002	0.065	609.0	0.002	0.063	F op bend
5	419*	408.3	0.026	0.103	399.5	0.026	0.168	collective
4	314 ± 2*	311.0	0.011	0.461	295.3	0.007	0.399	Me−OH torsion
3	NO	251.7	0.008	0.747	242.4	0.005	0.738	Me−OH torsion
2	163 ± 2	148.9	0.027	0.006	148.0	0.031	0.004	Me op bend
1	NO	63.9	0.011	0.025	63.0	0.014	0.011	Me torsion

[a] Raman (R) and IR intensities are expressed in units of the *Skew 3* mode #26 Raman intensity (= 109.0 A^4/amu) and #15 IR intensity (= 110.9 KM/mol), respectively. Frequencies obtained in toluene are marked with "*". Fundamentals, which could not be observed are marked "NO" or, when not reliably resolved, with "NR". Frequency errors are 1 cm^{-1} unless otherwise stated. "F" and "Me" Represent the furan ring and methanol parts of FA, respectively. In-plane and out-of-plane vibrations with respect to the furan ring are abbreviated "ip" and "op", respectively.

The root-mean-square (RMS) error of ν_{Calc} from experimental frequencies does not exhibit a significant dependency on the basis set used for the harmonic part. The largest absolute error is noted for the Me−CH stretching mode (#28), which is underestimated by 6-31G(d,p): 74 cm^{-1}, B1: 65 cm^{-1}, B2: 75 cm^{-1}, and B2a: 68 cm^{-1}. From Table 2, it is noted that large frequency errors appear to correlate with large frequency shifts of a normal mode between the different conformers. If normal mode #28 is omitted, the RMS error attains the values 6-31G(d,p): 10.0 cm^{-1}, B1: 10.3 cm^{-1}, B2: 8.4 cm^{-1}, and B2a: 10.4 cm^{-1}. If only the *Skew 1* conformer is considered ($p_1 = 1$, $p_2 = 0$, #28 omitted), the RMS error attains the values 6-31G(d,p): 12.4 cm^{-1}, B1: 12.1 cm^{-1}, B2: 9.8 cm^{-1}, and B2a: 11.6 cm^{-1}. In Table 2, we list the optimal (B2: 8.4 cm^{-1} error) hybrid frequencies of FA for each of the two lowest energy conformers, together with the experimental frequencies.

To examine the origin of these errors, anharmonic frequency calculations were performed for methanol using both B3LYP/6-31G(d,p) and MP2/6-31G(d,p). Excluding the lowest-frequency CH stretching mode, the anharmonic frequency corrections differed for each normal mode on average by 5 cm^{-1} between these methods, where the two largest deviations were for the lowest-frequency mode (27 cm^{-1}) and the next-lowest CH stretching mode (13 cm^{-1}). The lowest-frequency CH stretching mode attained, however, a correction of −331 cm^{-1} (B3LYP) and −76 cm^{-1} (MP2), respectively. Neither of the two calculations included a Fermi resonance treatment for this mode.

Discussion

The present work qualitatively confirms the existence and (Φ_1, Φ_2) values of five different FA conformers,[9] two of which have markedly lower free energy than the remaining three. The structural discrepancies between B3LYP and MP2 conformations, noted especially for the *Syn 2* (Φ_1, Φ_2) values, may be due to the better MP2 level description of long-range dispersion forces, but the relatively poor-quality basis set used for the MP2 calculations makes comparisons difficult. The calculated B3LYP dipole moments show for all the large basis sets consistently the same ordering of magnitudes as the MP2/6-31G(d) results, where *Skew 1* and *Skew 3* have the largest values.

Both the MP2/6-31G(d) as well as the present B3LYP calculations identify the *Skew 3* ($\Phi_1 = 106°$, $\Phi_2 = 60°$) as the lowest energy conformer. The present work reports free energies, whereas the previous MP2 work reports only the SCF energies. As opposed to the previous calculations, the B3LYP/B2a calculations do not identify the *Syn 1* but rather the *Skew 1* (107°, −53°) as the next-lowest energy conformer $\Delta G_{rel} = 43 \times 10^{-5}$ Hartree (= 1.1 kJ/mol) in much better accordance with experimental observations ($\Delta G_{rel} = 1.5 \pm 0.4$ kJ/mol).[9] The third-lowest energy conformer *Syn 1* (23°, 58°) has $\Delta G_{rel} = 133 \times 10^{-5}$ Hartree (= 3.5 kJ/mol), and does thus, together with experimental observations,[9] indicate that the MP2 result of 0.5 kJ/mol was underestimated. This also holds for the more comparable SCF energies, where the B3LYP/B2a calculation for *Syn 1* yields $\Delta E_{rel} = 150 \times 10^{-5}$ Hartree. These conclusions

are also confirmed by the hybrid ΔG values obtained from the (thermally corrected) MP2/B2a single-point energies.

The B3LYP calculations indicate, irrespective of basis set, that *all* FA conformations are significantly populated (>5% occupancy) at $T = 298$ K. Thus, none of them can be neglected in reaction rate considerations. This is a consequence of the fact that the ΔG_{rel} values of all five conformers in a vacuum are of the same order of magnitude as the value $k_B T = 94 \times 10^{-5}$ Hartree = 2.5 kJ/mol at $T = 298$ K. This is likely also the case in weakly interacting environments. For increased temperatures, that is, during the curing process, the occupational probabilities change, and the higher energy conformers become relatively more dominant. The thermodynamic and dipole moment results suggest that the ΔG_{rel} ordering of the five conformational states may depend on the polarity of the environment. It is notable that the largest dipole moment *Skew 1* conformer has a free energy relatively close to that of *Skew 3*. The *Skew 1* conformer could thus in a *polar* environment be more stable than *Skew 3*, which—due to its intramolecular hydrogen bond—has a reduced propensity for intermolecular hydrogen-bond formation. The *Skew 1* conformer can be relatively more stabilized both by specific hydrogen bonding to hydrogen-bond acceptors (e.g., water molecules) and by nonspecific dipolar interaction with the environment. The same effects can, of course, also be envisaged for the *Skew 2* and Syn conformers. These do, however, already pay an energy "penalty" with free energies of $>90 \times 10^{-5}$ Hartree above that of *Skew 1*, and it is thus not likely that hydrogen bonding will change their energies relative to that of *Skew 1*.

The inclusion of occupational probabilities leads to a small error improvement ($\sim$1−2 cm^{-1}) of the frequency calculations, which suggests that experimental bands contain contributions from several conformers. Interestingly, a rather large RMS frequency error contribution arises from the Me−CH stretching mode (#28). The anharmonic frequency calculations for methanol—comparing the MP2 and B3LYP methods for this purpose—suggest that a high level of ab-initio theory is needed for obtaining correct anharmonic frequencies for the CH stretching modes of the alcohol group. A recent work on the force field of methanol thus uses MP4 anharmonic calculations and demonstrates that the CH stretching mode frequencies are particularly sensitive to Fermi interactions, which upshifts the unperturbed lowest-frequency CH stretching mode by $\sim$50 cm^{-1}.[20] A threshold in excess of 100 cm^{-1} for resonance analysis was needed for proper convergence of these frequencies. Thus, the neglect of Fermi interactions for mode #28 (none were found within the 10-cm^{-1} threshold used by the Gaussian program) pertaining to the alcohol group may also contribute to the estimation error of this mode.

The issues of the environmental dependency of FA conformer occupation levels and the possible limitations of DFT anharmonic frequency calculations await future investigations.

Conclusion

The B3LYP method has been used to describe the thermodynamics of FA conformers in a vacuum or weakly interacting environments. Irrespective of the basis set used, all five FA conformers are populated at more than 5% probability level, and the lowest free energy *Skew 3* (B2a: 46%) and *Skew 1* (B2a: 30%) conformers are markedly more probable than the remaining three. MP2/B2a single-point energies obtained for the B3LYP/B2a structures confirmed these results. Hence, FA reactions such as self-condensation (polymerization) occur initially from all five conformers appropriately weighted by their respective population level, which likely is sensitive to the nature of the environment. The MP2 method used previously for estimating the thermodynamics of FA conformers in a vacuum may have suffered from basis set limitations as a rather limited size basis set was used.

When a single normal mode is omitted, the experimental and calculated B3LYP hybrid frequencies differ by a RMS error of 8 cm^{-1}, whereby a qualitative assignment of most FA normal mode vibrations is allowed for. The failure of the B3LYP frequency calculation to predict the omitted Me−CH stretching mode frequency results likely from a combination of (1) insufficient level of theory, where, for example, the MP*x* methods to a sufficient order (*x*) would be more appropriate, and (2) the neglect of Fermi interactions.

Acknowledgment. S.B. thanks the ECOBINDERS project ("Furan and lignin based resins as eco-friendly and durable solutions for wood preservation, panel, board and design products", call FP6-2003-NMP-SME-3) for financial support.

References and Notes

(1) Choura, M.; Belgacem, N. M.; Gandini, A. *Macromolecules* **1996**, *29*, 3839.
(2) Principe, M.; Ortiz, P.; Martinez, R. *Polym. Int.* **1999**, *48*, 637.
(3) Chuang, I. S.; Maciel, G. E.; Myers, G. E. *Macromolecules* **1984**, *17*, 1087.
(4) Gonzalez, R.; Martinez, R.; Ortiz, P. *Makromol. Chem.*—Macromol. Chem. Phys. **1992**, *193*, 1.
(5) Gonzalez, R.; Figueroa, J. M.; Gonzalez, H. *Eur. Polym. J.* **2002**, *38*, 287.
(6) Lande, S.; Eikenes, M.; Westin, M. *Scand. J. For. Res.* **2004**, *19*, 14.
(7) Lande, S.; Westin, M.; Schneider, M. *Scand. J. For. Res.* **2004**, *19*, 22.
(8) Leonov, A.; Marstokk, K. M.; de Meijere, A.; Mollendahl, H. *J. Phys. Chem. A* **2000**, *104*, 4421.
(9) Marstokk, K. M.; Mollendal, H. *Acta Chem. Scand.* **1994**, *48*, 25.
(10) Barone, V. *J. Phys. Chem. A* **2004**, *108*, 4146.
(11) Barone, V.; Festa, G.; Grandi, A.; Rega, N.; Sanna, N. *Chem. Phys. Lett.* **2004**, *388*, 279.
(12) Barone, V. *Chem. Phys. Lett.* **2004**, *383*, 528.
(13) Burcl, R.; Handy, N. C.; Carter, S. *Spectrochim. Acta, Part A—Mol. Biomol. Spectrosc.* **2003**, *59*, 1881.
(14) Boese, A. D.; Klopper, W.; Martin, J. M. L. *Int. J. Quantum Chem.* **2005**, *104*, 830.
(15) Boese, A. D.; Klopper, W.; Martin, J. M. L. *Mol. Phys.* **2005**, *103*, 863.
(16) Barone, V. *J. Chem. Phys.* **2005**, *122*, 014108.
(17) ASTM Standard guide for Raman shift standards for Raman spectroscopy, E1840. In *Annual Book of ASTM Standards*, ASTM: Philidelphia, 1996; pp 859−867.
(18) Berg, R. W.; Nørbygaard, T. *Appl. Spectrosc. Rev.* **2006**, *41*, 165.
(19) Frisch, M. J.; Trucks, G. W.; Schlegel, H. B.; Scuseria, G. E.; Robb, M. A.; Cheeseman, J. R.; Montgomery, J. A., Jr.; Vreven, T.; Kudin, K. N.; Burant, J. C.; Millam, J. M.; Iyengar, S. S.; Tomasi, J.; Barone, V.; Mennucci, B.; Cossi, M.; Scalmani, G.; Rega, N.; Petersson, G. A.; Nakatsuji, H.; Hada, M.; Ehara, M.; Toyota, K.; Fukuda, R.; Hasegawa, J.; Ishida, M.; Nakajima, T.; Honda, Y.; Kitao, O.; Nakai, H.; Klene, M.; Li, X.; Knox, J. E.; Hratchian, H. P.; Cross, J. B.; Bakken, V.; Adamo, C.; Jaramillo, J.; Gomperts, R.; Stratmann, R. E.; Yazyev, O.; Austin, A. J.; Cammi, R.; Pomelli, C.; Ochterski, J. W.; Ayala, P. Y.; Morokuma, K.; Voth, G. A.; Salvador, P.; Dannenberg, J. J.; Zakrzewski, V. G.; Dapprich, S.; Daniels, A. D.; Strain, M. C.; Farkas, O.; Malick, D. K.; Rabuck, A. D.; Raghavachari, K.; Foresman, J. B.; Ortiz, J. V.; Cui, Q.; Baboul, A. G.; Clifford, S.; Cioslowski, J.; Stefanov, B. B.; Liu, G.; Liashenko, A.; Piskorz, P.; Komaromi, I.; Martin, R. L.; Fox, D. J.; Keith, T.; Al-Laham, M. A.; Peng, C. Y.; Nanayakkara, A.; Challacombe, M.; Gill, P. M. W.; Johnson, B.; Chen, W.; Wong, M. W.; Gonzalez, C.; Pople, J. A. *Gaussian 03*, Revision C; Gaussian, Inc.: Wallingford, CT, 2004.
(20) Miani, A.; Hänninen, V.; Horn, M.; Halonen, L. *Mol. Phys.* **2000**, *98*, 1737.